Surface & Coatings Technology 206 (2012) 4601–4605

Effect of a bioactive glass-ceramic on the apatite nucleation on titanium surface modified by micro-arc oxidation

Paulo Soares [a,*], Carlos A.H. Laurindo [a], Ricardo D. Torres [a], Neide K. Kuromoto [b], Oscar Peitl [c], Edgar D. Zanotto [c]

[a] Mechanical Engineering Department, Polytechnic School, Pontifícia Universidade Católica do Paraná, 80215-901 Curitiba (PR), Brazil
[b] Physics Department, Universidade Federal do Paraná, 81531-990 Curitiba (PR), Brazil
[c] Materials Engineering Department, Universidade Federal de São Carlos, 13565-905 São Carlos (SP), Brazil

ARTICLE INFO

Article history:
Received 5 November 2011
Accepted in revised form 5 May 2012
Available online 14 May 2012

Keywords:
Bioactive glass-ceramic
Titanium
Micro-arc oxidation
Hydroxyapatite formation

ABSTRACT

The aim of this work was to evaluate the ability of a bioactive glass-ceramic to induce the apatite nucleation on the titanium oxide layer produced by micro-arc oxidation. "*In vitro*" tests were carried out on a simulated body fluid solution in two different manners: one group was soaked in the SBF, while the other group was soaked together with the bioactive glass-ceramic. Results revealed that after 7 days, the specimens soaked in SBF were covered with an amorphous calcium phosphate layer, while the specimens soaked in SBF plus glass-ceramic formed a crystalline apatite layer, suggesting thus, that the glass-ceramic provides silanol groups that accelerated the hydroxyapatite apatite precipitation on the anodic TiO_2 layer.

1. Introduction

Bioactive ceramics such as Bioglass [1], Cerabone A/W [2], and Biosilicato [3], have the properties to spontaneously bond and integrate with living bone forming a biologically active bone-like apatite layer on their surfaces. But they are not appropriate to replace bones when subjected to load due to their poor mechanical properties [4]. On the other hand, the use of titanium and its alloys are widely used in biomedical devices due to its good biocompatibility, corrosion resistance, good fatigue strength, high fracture toughness and elastic modulus near to that of human cortical bones [5]. However, Ti and its alloys are *not* bioactive [6]. To improve the bone bonding ability of titanium implants, several methods have been used to modify the titanium surfaces including deposition of bioactive coatings [7]. One of the most accepted and commercialized bioactive coating material is the hydroxyapatite (HA) applied by plasma spray [8], but its final composition, as well as its adhesion to substrate, is not well controlled [9]. Bioglass coatings deposited by plasma spray or enameling fail due to the poor adhesion of the coating and/or degradation of the glass properties during the coating procedure [10,11].

Another technique extensively used to improve the surface interaction of titanium with living tissues is the micro-arc oxidation (MAO). Using this technique, it is possible to obtain a tailored surface, with desired roughness, composition and porous size, by controlling the electrolyte, applied voltage and/or current, and oxidation time [12–18]. Besides the improvement of osseointegration, such surfaces may enhance the anchorage of bioceramics coatings.

The mechanism of apatite formation on the modified titanium has attracted considerable interest, once it may provide information about bioactive surface functionalization of non-bioactive materials. It is known that the mechanism of apatite formation on these bioceramics depends on the corrosion and precipitation processes leading to the formation of functional groups when soaked in a simulated body fluid (SBF). These groups have specific structures with negative charges, and induce apatite formation via formation of an amorphous calcium phosphate [19–21]. The fundamental understanding of this mechanism provides the guidelines for designing novel bioactive materials with different surface properties.

The aim of this study was to evaluate the ability of a bioactive glass-ceramic as an induction agent for the formation of apatite layer on oxidized titanium samples when soaked in simulated body fluid (SBF). This work will give us a better understanding of how the application of the glass-ceramic acts as a bioactive coating on an anchoring substrate such as porous titanium oxide layer.

2. Material and methods

Commercially pure titanium (cp-Ti) plates (20×10×0.9) mm, ASTM grade 2, were mechanically ground using #1000 SiC paper,

* Corresponding author at: Pontifícia Universidade Católica do Paraná, PUCPR, Escola Politécnica, Departamento de Engenharia Mecânica, ParqTec, Bloco III, Rua Imaculada Conceição. 1155, Prado Velho, 80215-901, Curitiba, PR, Brazil. Tel.: +55 41 3271 1346; fax: +55 41 3271 1349.
E-mail address: pa.soares@pucpr.br (P. Soares).

0257-8972/$ – see front matter © 2012 Elsevier B.V. All rights reserved.
doi:10.1016/j.surfcoat.2012.05.019

then ultrasonically cleaned with acetone, followed by distilled water rinsing. The anodic oxidation was carried out at the center of the specimens under potentiostatic mode with an applied voltage of 110 V for 1 min at room temperature, using 1 M Na_2SO_4 solution as the electrolyte, and a platinum plate as a counter electrode.

In order to test the ability of the bioactive glass-ceramic as an inducing agent of apatite formation, the oxidized specimens were divided into two groups and soaked in simulated body fluid (SBF). The SBF was prepared by dissolving reagent grade NaCl, $NaHCO_3$, KCl, $K_2PO_4.3H_2O$, $MgCl_2.6H_2O$, $CaCl_2$, and Na_2SO_4 into deionized water, and buffered at pH 7.25 with tris-hydroxymethyl aminomethane [$(CH_2OH)_3CNH_2$] and hydrochloric acid [19]. Group 1 consisted only of oxidized Ti specimens (surface area of 4.5 cm²); and Group 2 of the oxidized Ti specimens plus a small rod (total surface area of 7.5 cm²) of a fully crystallized Na_2O-CaO-SiO_2-P_2O_5 bioactive glass-ceramic. The detailed glass-ceramic production is described elsewhere [3,22,23]. Both groups were soaked in SBF at 37 °C for 7 days. The distance between the oxidized area and the glass-ceramic inside the recipient was 3 mm. About 45 ml of SBF for Group 1 and 75 ml of SBF for Group 2 were added to the container to give a ratio of the samples surface area per volume (SA/V) of 0.1 cm^{-1} [19].

The specimens surface was evaluated by scanning electron microscopy (SEM, Jeol JSM-6360LV). The qualitative composition of the surface layer was analyzed by energy dispersive spectroscopy (EDS, Thermo Noran). Surface structural changes of the anodic layers were determined by X-ray diffraction (XRD, Shimadzu XRD-7000) using the Bragg–Bretano method with Cu radiation at 40 kV and 30 mA, and Fourier Transformed Infrared Spectroscopy using the reflectance mode (FTIR, Perkin Elmer Spectrum GX). Spectra were obtained between 4000 and 400 cm^{-1} at 2 cm^{-1} resolution.

3. Results

Fig. 1 shows a porous and rough surface with irregular morphology of the TiO_2 layer produced in 1.0 M Na_2SO_4 electrolyte. The anodization process starts with the current instantly reaching a maximum value (1.5A) and then decreasing to a nearly constant value of 300 mA until the end of the process, after 1 min. At the potential of 110 V, we observed a sparking phenomenon during anodization due to the dielectric breakdown of the oxide layer, characterized by a voltage fluctuation [24,25]. X-ray diffraction (XRD) patterns (Fig. 2) showed that the oxide layer on the titanium surface consisted of the rutile phase.

After 7 days soaked in SBF solution, the surface of Group 1 samples was totally covered with a thin layer rich in Ca and P as observed by SEM/EDS (Fig. 3a–d). EDS results also showed Ti and O peaks, suggesting that it is a very thin calcium phosphate layer. XRD patterns of the Group 1 specimens (not shown here) exhibited no other peaks,

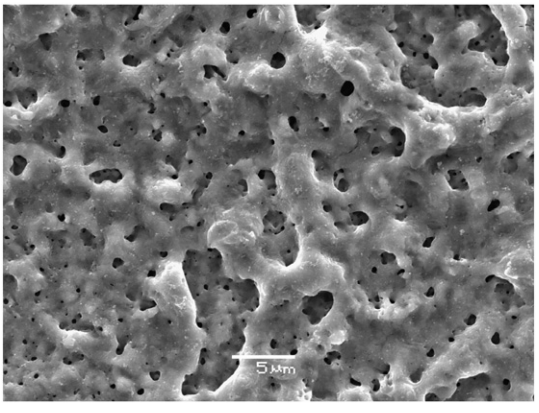

Fig. 1. Morphology of the TiO_2 layer produced by anodic oxidation with 1 M Na_2SO_4 electrolyte under potentiostatic mode on cp-Ti. Bar denotes 5 µm.

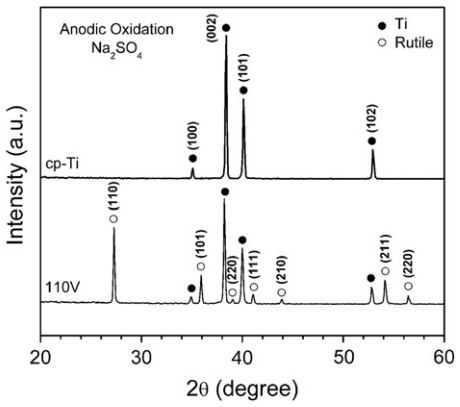

Fig. 2. XDR patterns of the cp-Ti surface, and anodic oxidized layer produced at 110 V in 1 M Na_2SO_4 electrolyte.

except for the diffraction peaks from rutile and titanium. As pointed out by Kokubo et al. [6], this amorphous calcium phosphate layer will be transformed into crystalline apatite after a longer soaking period.

The morphology of the Group 2 specimens soaked in SBF with glass-ceramic for 7 days is shown in Fig. 4. This set of micrographs shows the TiO_2 surface changes as a function of the distance to the glass-ceramic. First, the region that is farthest (about 10 mm) from the glass-ceramic rod (Fig. 4a) shows that the surface is not altered. As the distance between the anodic layer and the glass-ceramic rod decreases, small spherical particles are formed all over the porous surface with no preferential site for nucleation, and the number and size of those particles increase. It is interesting to note that the spheres are also formed inside the layer pores, and they grow, unite, and cover the entire surface (Fig. 4b–f). The EDS spectrum shows that these spheres contain calcium and phosphorus, along with Si and Mg from the interaction with the bioactive glass-ceramic and SBF. At regions far from the bioactive glass-ceramic we observed only Ti and O.

Fig. 5 shows the FTIR spectra of the Group 2 specimens surface before and after soaked in SBF for 7 days. The measurements were done in two different regions, near and far from the glass-ceramic rod. It is observed that the spectrum of the TiO_2 layer before the exposure to SBF has an almost identical profile to the spectrum of the TiO_2 layer region soaked in SBF far from the bioactive glass-ceramic. Nevertheless, the spectrum of the region near the glass-ceramic exhibits a very different profile, indicating remarkable surface changes. Note that this spectrum shows reflectance bands on wavenumbers very close to the ones exhibited by the layer formed on the glass-ceramic surface after soaked in SBF for 7 days. The band assignments around 515 cm^{-1}, 560 cm^{-1} and 600 cm^{-1} correspond to P-O bending due to the apatite formation.

4. Discussion

The mechanism of apatite formation on the titanium oxide layer produced by anodic oxidation was described by several authors (see for example, Wei et al. [26] and Kokubo [27]) as follows: immediately after soaking in SBF, the Ti-OH groups on the surface are dissociated into negatively charged units of $Ti\text{-}O^-$ owing to its isoelectric point, which is lower than the pH of SBF. Next, this $Ti\text{-}O^-$ units combine with positively charged Ca^{2+} ions from SBF forming an amorphous calcium titanate. The positively charged calcium titanate interacts with the negatively charged phosphate ions from the fluid forming an amorphous calcium phosphate. As the reaction continues, the amorphous calcium phosphate crystallizes into bone-like apatite.

We believe that the amorphous calcium phosphate formed on the oxidized layer (Fig. 3) did not reach the conditions to evolve, get

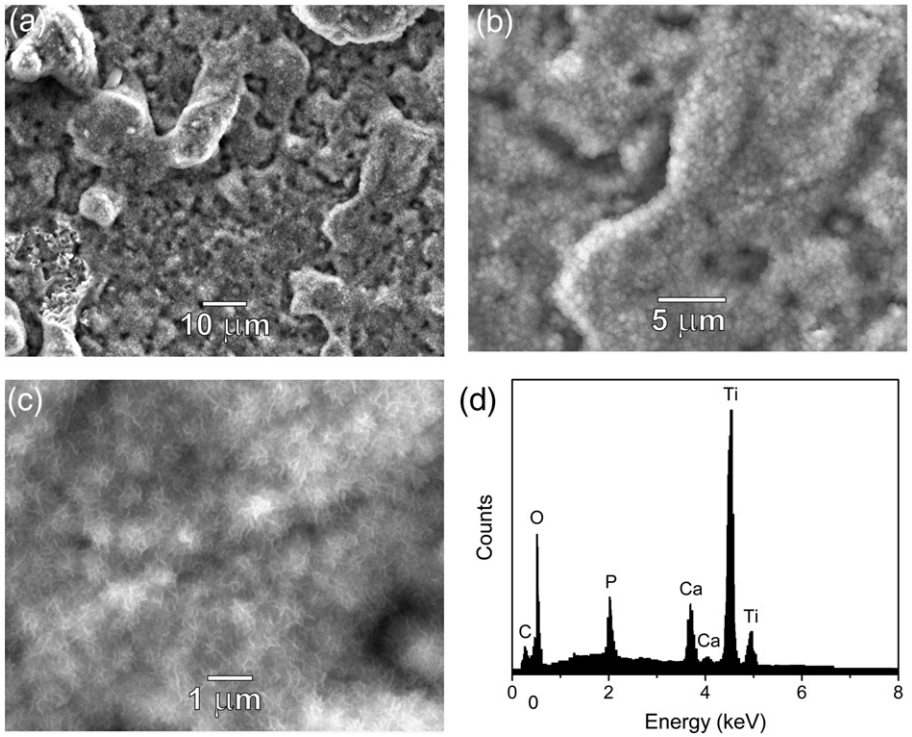

Fig. 3. Morphology of the amorphous Ca-P layer on Group 1 samples surface soaked for seven days in SBF solution, with different magnification (a–c) and EDS spectrum (d).

thicker and crystallize into a well-developed apatite layer, as observed in the work of Kawashita et al. [28] for the same kind of oxide surface. A possible explanation is that the ion supply of the SBF solution was not enough to induce such transformation during the period of 7 days. On the other hand, samples from Group 2 have shown a notably different result, with the presence of typical crystalline apatite spheres.

Some authors have drawn attention to the importance of dissolution products of bioactive glasses and silica in the enhancement of bone formation, gene activation, and apatite formation *in vitro* and *in vivo* [29–34].

The process of apatite formation on the glass surface was investigated by several authors [35–37] and can be summarized as follows:

(i) First, the Na^+ ions of the glass surface change place with the H^+ or H_3O^+ ions of the solution;
(ii) There is an OH^- concentration increase of the solution, increasing its pH, which causes the breakdown of the Si-O-Si network of the glass and the release of $Si(OH)_4$ in the solution;
(iii) Repolymerization of the $Si(OH)_4$ on the glass surface in the form of a nanoporous silica-gel layer;

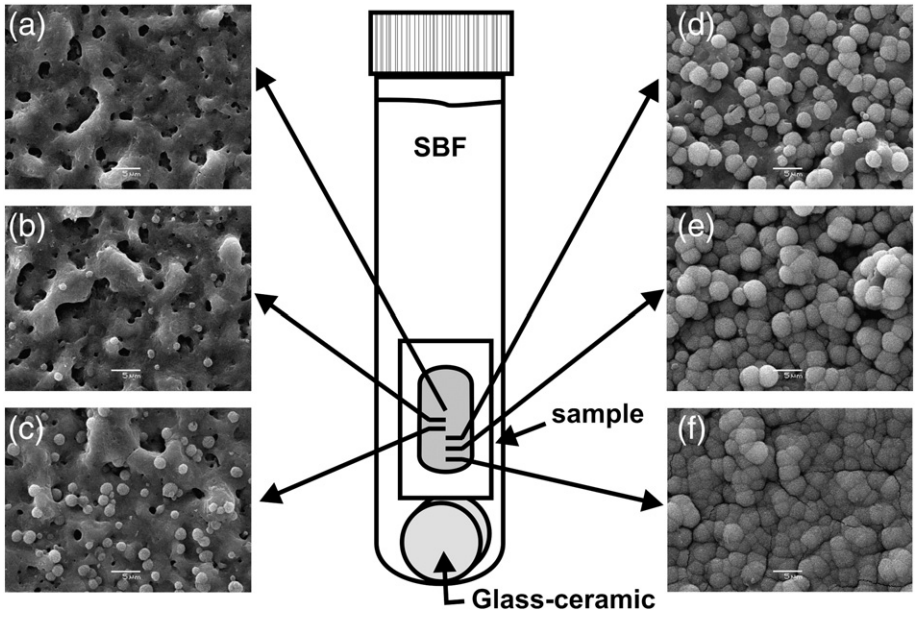

Fig. 4. SEM micrographs showing the apatite formation on TiO_2 layer as a function of the distance to glass-ceramic rod. The last micrograph (f) is the nearest to the glass-ceramic rod. Bars denote 5 μm.

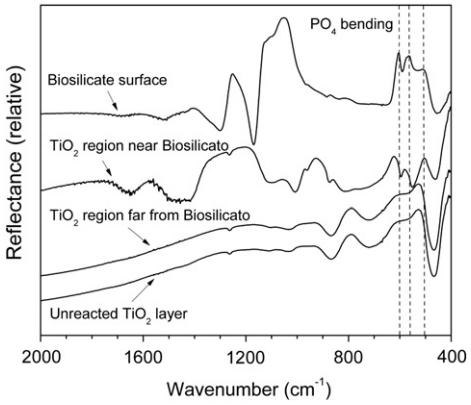

Fig. 5. FTIR spectra of the Group 2 specimens surface and glass-ceramic surface before (unreacted TiO_2 layer) and after soaked in SBF for 7 days.

(iv) Precipitation of calcium and phosphate ions on the porous silica-gel layer forming an amorphous calcium phosphate layer;
(ii) Finally, the amorphous calcium phosphate stabilizes into crystalline apatite and grows spontaneously.

If we look at the micrograph of a specimen from Group 2 (Fig. 4a), the amorphous calcium phosphate layer is not observed as in Group 1 (Fig. 3). The crystalline apatite is nucleated directly on the TiO_2 layer, induced by the glass-ceramic. The reason for this difference is that there is an increase of the OH^-, calcium and phosphate concentration, supplied by the glass-ceramic, and it is also due to the introduction of a new component, which was not present before in the solution, $Si(OH)_4$, which favors the silica-gel formation. The presence of $Si(OH)_4$ and the increase of the OH^- concentration are the main factors which lead to the nucleation and growth of apatite on the TiO_2 layer. Similar results were found by Kokubo et al. [38]. They observed that the calcium and silicate ions, added to a SBF solution, induced the formation of apatite layer on a non-bioactive glass-ceramic. They suggested that the silicate ions provide favorable sites for the apatite nucleation.

We suggest that the reaction of Ti-OH with $Si(OH)_4$ groups on the anodized surface is the first step for apatite nucleation according to the following reaction:

$$Ti-OH + HO-Si(OH)_3 \rightarrow Ti-O-Si(OH)_3 + H_2O \quad (1)$$

The silanol group attached to the TiO_2 surface may react with 3 other silanol groups, which can keep reacting with other silanol groups forming a network of hydrated silica oligomer, forming the substrate which will combine with hydrated calcium and phosphate complexes to generate the active sites for the nucleation of apatite.

Sahai and Anseau [39] have used crystallographic constraints with molecular orbital calculations to study the nucleation of apatite on Pseudowollastonite (psW) bioceramic. They identified the active site and proposed the reaction mechanism for the heterogeneous nucleation of the earliest calcium phosphate oligomer phase. According to their calculations, a cyclic trimmer with 3 silanol groups (Si_3O_9) arranged at 60° to each other provides a stereochemical match for O atoms bonded to Ca^{2+} on the (001) face of the hydroxyapatite.

The presence of glass-ceramic near the TiO_2 layer provides the conditions to enable the mechanism described above. The glass-ceramic releases a high concentration of $Si(OH)_4$ groups, which provide a critical active site density. The hydrated calcium complex and the hydrated hydrogen phosphate ions are already present in the SBF and may also be released from the glass-ceramic surface. This conclusion is supported by the fact that the density of apatite crystals in the vicinity of the glass-ceramic is high and decreases as the distance increases.

As there is a lack of $Si(OH)_4$ groups in the solution for the specimens in Group 1, the condition is not favorable for apatite crystals nucleation. Another advantage of the glass-ceramic is that it might increase the pH due to the Na^+ exchange of the material with H^+ ions of the solution, which results in the increase of the OH^- concentration, inducing the apatite nucleation.

An interesting observation about the cp-Ti surface outside the anodized region is that this surface near the glass-ceramic did not show apatite nucleation. Hence, non-modified Ti does not react with the silanol groups and, therefore, there is no formation of active sites for apatite nucleation and growth. This result indicates that the anodic layer is bioactive and that the non-oxidized surface is not. Thus, the bioactive glass-ceramic is very important to induce the apatite nucleation and accelerate apatite formation on surfaces that present bioactivity.

We can summarize the importance of bioactive glass-ceramic for apatite formation on the anodic layer:

(i) the nucleation of apatite occurred only on the MAO layer and more intensely near the glass-ceramic rod (Figs. 4 and 5);
(ii) as the distance between the glass-ceramic and the MAO layer increases, the number of the apatite nucleation sites decreases (Fig. 5). At the opposite side of the MAO layer, far from the glass-ceramic, no apatite was observed on the oxidized surface;
(iii) in the non-modified Ti region, that was not anodized and was near the glass-ceramic, no apatite formation was observed.

These results have shown a way to accelerate the apatite formation on a titanium oxide layer produced by anodic oxidation. The crystalline apatite layer was observed only on specimens soaked with the glass-ceramic in the solution, while the specimens without the glass-ceramic, submitted to the same incubation time show a surface with an amorphous calcium phosphate layer, which, according to Jonásová, is the step prior to apatite formation [40]. According to Kokubo [41], an essential requirement for the implants to bond to living bone is the formation of a biologically active bone-like apatite layer on their surfaces in the body, and that this apatite layer can be reproduced *in vitro* when soaked in simulated body fluid. Thus, it is expected that the same reaction forming the bone-like apatite that occurred on MAO surfaces with the presence or not of the glass-ceramic could occur in the living body.

Therefore, in order to change a biocompatible titanium surface into a bioactive surface, it is necessary to make some chemical and microstructural modifications such as the micro-arc oxidation, and an improvement of its bioactivity is possible by adding a source of silanol groups such as the ones provided by the glass-ceramic.

5. Conclusions

The nucleation of apatite induced by a bioactive glass-ceramic was studied using SEM/EDS and FTIR. Specimens of micro-arc oxidized titanium were soaked in SBF for 7 days without (Group 1) and with (Group 2) the addition of a bioactive glass-ceramic rod. For this period, specimens from Group 1 presented an amorphous calcium phosphate layer, while the specimens from Group 2 presented hydroxyapatite crystals, with different nucleation density as a function of the distance from the glass-ceramic. The addition of a bioactive glass-ceramic rod into the SBF provided a source of $Si(OH)_4$ groups in the solution, induced apatite nucleation and accelerated apatite growth on the MAO layer near the glass-ceramic. The nearest the surface layer was to the bioactive glass-ceramic the more apatite was formed.

Acknowledgments

The authors thank the Paraná State Funding Agency (Fundação Araucária) and Conselho Nacional de Pesquisa (CNPq) for the financial support, and the Electron Microscopy Center at UFPR for using their facilities.

References

[1] L.L. Hench, J. Am. Ceram. Soc. 81 (1991) 1497.
[2] T. Kokubo, S. Ito, S. Sakka, T. Yamamuro, J. Mater. Sci. 21 (1986) 536.
[3] O. Peitl-Filho, E.D. Zanotto, L.L. Hench, J. Non-Cryst. Solids 292 (2001).
[4] T. Kokubo, Biomaterials 12 (1991) 155.
[5] M. Geetha, A.K. Singh, R. Asokamani, A.K. Gogia, Prog. Mater. Sci. 54 (2009) 397.
[6] T. Kokubo, H.M. Kim, M. Kawashita, Biomaterials 24 (2003) 2161.
[7] X. Liu, P.K. Chu, C. Ding, Mater. Sci. Eng. Rep. 47 (2004) 49.
[8] P.L. Tranquilli, A. Merolli, O. Palmacci, J. Mater. Sci. Mater. Med. 5 (1994) 345.
[9] M. Roya, A. Bandyopadhyaya, S. Bose, Surf. Coat. Technol. 205 (2011) 2785.
[10] X. Liu, R.W.Y. Poon, S.C.H. Kwok, P.K. Chu, C. Ding, Surf. Coat. Technol. 186 (2004) 227.
[11] A. Pazo, E. Saiz, A.P. Tomsia, Acta Mater. 46 (1998) 2551.
[12] D.Q. Wei, Y. Zhou, D.C. Jia, Y.M. Wang, Acta Biomater. 3 (2007) 817.
[13] P. Soares, A. Mikowski, C.M. Lepienski, E. Santos-Jr, G.A. Soares, V. Swinka-Filho, N.K. Kuromoto, J. Biomed. Mater. Res. B 84B (2008) 524.
[14] Y. Han, S. Hong, K. Xu, Surf. Coat. Technol. 168 (2003) 249.
[15] T. Kokubo, H.M. Kim, M. Kawashita, T. Nakamura, J. Mater. Sci. Mater. Med. 15 (2004) 99.
[16] B.C. Yang, M. Uchida, H.M. Kim, X.D. Zhang, T. Kokubo, Biomaterials 25 (2004) 1003.
[17] Y. Yan, J. Sun, Y. Han, D. Li, K. Cui, Surf. Coat. Technol. 205 (2010) 1702.
[18] Y.T. Sul, C.B. Johansson, Y. Jeong, K. Roser, A. Wennerberg, T. Albrektsson, J. Mater. Sci. Mater. Med. 12 (2001) 1025.
[19] T. Kokubo, H. Kushitani, S. Sakka, T. Kitsugi, T. Yamamuro, J. Biomed. Mater. Res. 24 (1990) 721.
[20] R.A. Martin, H. Twyman, D. Qiu, J.C. Knowles, R.J. Newport, J. Mater. Sci. Mater. Med. 20 (2009) 883.
[21] H.M. Kim, F. Miyaji, T. Kokubo, T. Nakamuta, J. Ceram. Soc. Jpn. 105 (1997) 111.
[22] E.D. Zanotto, C. Ravagnani, O. Peitl Filho, H. Panzeri, E.H. Guimarães Lara, Patent No. WO2004074199 (2004).
[23] J. Moura, L.N. Teixeira, C. Ravagnani, O. Peitl Filho, E.D. Zanotto, M.M. Beloti, H. Panzeri, A.L. Rosa, P.T. Oliveira, J. Biomed. Mater. Res. A 82A (2007) 545.
[24] S. Meyer, R. Gorges, G. Kreisel, Thin Solid Films 450 (2004) 276.
[25] A.L. Yerokhin, X. Nie, A. Leyland, A. Mattheus, S.J. Dowey, Surf. Coat. Technol. 122 (1999) 73.
[26] D. Wei, Y. Zhou, Y. Wang, Q. Meng, D. Jia, Surf. Coat. Technol. 202 (2008) 5012.
[27] T. Kokubo, Acta Mater. 46 (1999) 2519.
[28] M. Kawashita, X.Y. Cui, H.M. Kim, T. Kokubo, T. Nakamura, Key Eng. Mater. 254 (2004) 459.
[29] P. Ducheyne, Q. Qiu, Biomaterials 20 (1999) 2287.
[30] L.L. Hench, J.M. Polak, I.D. Xynos, L.D.K. Buttery, Mater. Res. Innov. 3 (2000) 313.
[31] I.D. Xynos, A.J. Edgar, L.D. Buttery, L.L. Hench, J.M. Polak, J. Biomed. Mater. Res. 55 (2001) 151.
[32] L.L. Hench, I.D. Xynos, A.J. Edgar, L.D.K. Buttery, J.M. Polak, J.P. Zhong, X.Y. Liu, J. Chang, J. Inorg. Mater. 17 (2002) 897.
[33] K.H. Karlsson, Glass Technol. 45 (2004) 157.
[34] K.A. Hing, P.A. Revell, N. Smith, T. Buckland, Biomaterials 27 (2006) 5014.
[35] C.Y. Kim, A.E. Clark, L.L. Hench, J. Non-Cryst. Solids 113 (1989) 195.
[36] H. Takadama, H.M. Kim, T. Kokubo, T. Nakamura, J. Am. Ceram. Soc. 85 (2002) 1933.
[37] L.L. Hench, J. Am. Ceram. Soc. 74 (1991) 1487.
[38] T. Kokubo, H. Kushitani, C. Ohtsuki, S. Sakka, T. Yamamuro, J. Mater. Sci. Mater. Med. 4 (1993) 1.
[39] N. Sahai, M. Anseau, Biomaterials 26 (2005) 5763.
[40] L. Jonásová, F.A. Muller, A. Helebrant, J. Strnad, P. Greil, Biomaterials 25 (2004) 1187.
[41] T. Kokubo, Thermochim. Acta 280/281 (1996) 479.